Structure and Properties of Butadiene–*tert*-Butyl Methacrylate and Butadiene/Styrene–*tert*-Butyl Methacrylate Triblock Copolymer Ionomers

Don Loveday,[†] Garth L. Wilkes,*[,†] Craig D. Deporter,[‡] and James E. McGrath[‡]

Departments of Chemical Engineering and Chemistry and Polymer Materials and Interfaces Laboratory, Virginia Polytechnic Institute and State University, Blacksburg, Virginia 24061

Received September 28, 1994; Revised Manuscript Received August 8, 1995[⊗]

ABSTRACT: The structure–property behavior of two series of new ionomers derived from well-defined block copolymers was investigated. The two types of triblock systems were either poly(tBMA-*b*-BD-*b*-tBMA) or poly(tBMA-*b*-S-*t*-BD-*t*-S-*b*-tBMA) (tBMA = *tert*-butyl methacrylate; BD = butadiene; S = styrene; *t* = taper). The materials have been examined in the *tert*-butyl ester forms and also hydrolyzed (carboxylic acid) and neutralized to the cesium carboxylate salt. The ester precursor exhibits a morphological transformation upon neutralization in the case of a 9 mol % tBMA–BD triblock, from unoriented rodlike domains in the ester precursor to ion-containing spheroids in the ionomer. This transformation was observed by transmission electron microscopy (TEM) and also supported by the dynamic mechanical behavior of the respective systems. The introduction of styrene into the butadiene center block results in an increase in the glass transition temperature, as anticipated. However, the tapered nature of the center block in the styrenic materials promotes greater phase mixing, as supporting TEM and dynamic mechanical analysis (DMA) indicate. The composition of the center block in these tapered materials also alters the glass transition, as shown by DMA. In the tapered SBS cesium ionomers, the temperature of the transition to flow occurs at higher temperatures as the length of the ionic end block increases.

Introduction

Polymer properties can be altered by the incorporation of ionic species in the chain, and these changes are attributed to the aggregation of the ionic species into separate domains in the matrix. For less than ~15 mol % of ionized species attached to an otherwise low dielectric constant backbone, the polymers are termed ionomers. Several theories regarding the aggregation mechanism and subsequent morphological features of the ionic domain have been proposed.[1–9] These theories, which were developed from random ionomers, generally conflict with one another or predict structures exclusive of the observed properties (or vice versa), with the exception of Eisenberg's recent model.[9] However, interest has developed in precisely locating the ionic functionality on the chain, as in telechelic ionomers[10–14] and segmented ionomers.[15–17] These "well-defined" ionomers have been developed to control and study the nature and ordering of the ionic domains and, potentially, the properties of the system. In addition to the telechelics and segmented ionomers, interest has focused on the block ionomers, where all or part of one or more blocks is ionized. In these block ionomers, the ionization promotes an increased tendency toward phase separation through the addition of the Coulombic interaction of the ionic groups versus the nonionic analogous polymer.

McGrath et al.[18–26] pioneered many of the synthetic aspects of the block copolymer-based ionomers, such as those studied by Venkateshwaran and co-workers[27,28] and DePorter et al.[21,24] In the systems studied by Deporter and Venkateshwaran and co-workers, the block copolymer ionomers were prepared by first producing di- and triblock alkyl methacrylates by anionic methods. The nonionic blocks were either 2-ethylhexyl or *n*-hexyl methacrylate. The tBMA end block was then hydrolyzed, and the resultant methacrylic acid block was neutralized to afford either the cesium or the potassium ionomer.[24] These ionomers were characterized in terms of their structure and properties, exhibiting a rodlike or discontinuous lamellar structure in the case of the diblocks with 10 mol % ionic content in the fully neutralized end block and dispersed spherical ionic domains in the case of the triblocks of the same ionic content (i.e., 5 mol % in each fully ionized end block). The observation of rods and not spherical domains in the diblocks was surprising, considering that the ionic block was only 10 mol % of the system, much less than is typically needed for rodlike domains to form in nonionic block copolymers. The triblock ionomers of the same total end block content, on the other hand, exhibited dispersed spheroid morphology in transmission electron microscopy (TEM). The mechanical properties of the triblock materials, however, were unexpectedly like those of a pressure-sensitive adhesive rather than the desired elastomeric nature.[28]

Munk and co-workers have also synthesized poly(styrene-*b*-*tert*-butyl methacrylate) di- and triblock copolymers which were then hydrolyzed to poly(styrene-*b*-methacrylic acid).[29] These block copolymers were of narrow molecular weight distribution, with $\bar{M}_w/\bar{M}_n$ less than 1.1. The block copolymers and their acidic derivatives were characterized by thermogravimetry and differential scanning calorimetry.[29] It was found that the acidic derivative was less thermally stable than the ester precursor. The acidic form lost significant mass (by formation of anhydrides and water loss) up to 150 °C while the ester did not. The acidic materials were also used to consider the dynamics of micellization in water/dioxane solutions as block polyelectrolytes.[30,31] It was found that the dioxane-rich systems exhibited dynamic equilibrium, while in water-rich systems this equilibrium was "frozen".[30]

* Author to whom correspondence should be addressed.
[†] Department of Chemical Engineering.
[‡] Department of Chemistry.
[⊗] Abstract published in *Advance ACS Abstracts,* October 1, 1995.

0024-9297/95/2228-7822$09.00/0

Eisenberg and co-workers[32-37] extensively studied poly(4-vinylpyridinium-*b*-styrene-*b*-4-vinylpyridinium)-based triblock ionomers, where the end blocks are fully quaternized. Gauthier and Eisenberg[32] found a single T_g in these systems, that of the PS midblock. However, the T_g of the quaternary end blocks, presumed to be 200 °C, is well above the dequaternization temperature (~150 °C) of the end blocks and is not experimentally accessible. Wollmann, Williams, and Eisenberg studied "bottlebrush" ionomers,[33] where the poly(vinylpyridinium) end blocks are neutralized with iodoalkanes of different lengths, providing the "bristled" texture of the end block. In another study, Gouin et al.[34,35] found that the small-angle X-ray scattering (SAXS) from the PS–poly(4-vinylpyridinium) triblock ionomers with various methyl iodide quaternized end block lengths showed a broad asymmetric maximum (broader on the higher angle side). The location of the peak and peak maximum was a function of end block length. This maximum was interpreted to indicate periodic spacing between the ionic domains in terms of a paracrystalline lattice of ionic spheres. The authors also suggested, on the basis of the presence of a broad secondary SAXS peak, that the ionic domains could be "elongate" and spheroidal in shape (i.e., shape anisotropy). Though, as they note in their discussion, SAXS cannot easily differentiate between shape anisotropy and size distribution in a macroscopically unordered system. As well, the elongate spheroid domains would not seem to be as favorable as spheres if the morphology were to be the minimal energy state. Thus, it is not entirely certain that this method uniquely describes the morphology without conclusive evidence such as direct observation by TEM. A recent paper by Gouin et al.[34] compares the morphological features of a few block ionomer systems, including triblock ionomers of cesium methacrylate end blocks and poly(styrene) midblocks of various lengths, though no TEM results are presented.

Weiss and co-workers[38-41] studied partially sulfonated poly(styrene-*b*-ethene-*co*-butene-*b*-styrene) (SEBS) ionomers in which there are two levels of phase separation. The primary phase separation is between the polystyrene blocks and the poly(ethene-*co*-butene) block. The end blocks are random, lightly sulfonated (partially neutralized, up to 12 mol %) polystyrene ionomers with sodium or zinc counterions, and thus there is additional phase separation *within* the polystyrene domains. This ionic phase separation in the PS end block domains is evidenced by the appearance of a high-temperature dynamic mechanical transition and a second SAXS peak, both associated with the ionic domains dispersed in the PS domains. In their recent paper,[41] Weiss et al. stated that the morphology of solution-cast SEBS ionomers is lamellar, while that of compression-molded specimens is spherical. In either case, the morphology of the lightly sulfonated PS end blocks was found to be fit best by an interparticle SAXS scattering model, the modified hard-sphere model.

Deporter et al.[25,26] recently produced a series of triblock ionomers with elastomeric center blocks of butadiene or tapered styrene/butadiene/styrene (tSBS), in an effort to obtain better elastomeric properties than the previous, alkyl methacrylate systems.[24] This report describes the structure–property behavior of these triblock ionomer elastomers with emphasis on the effect of end block ionization, center block and end block length, and center block composition.

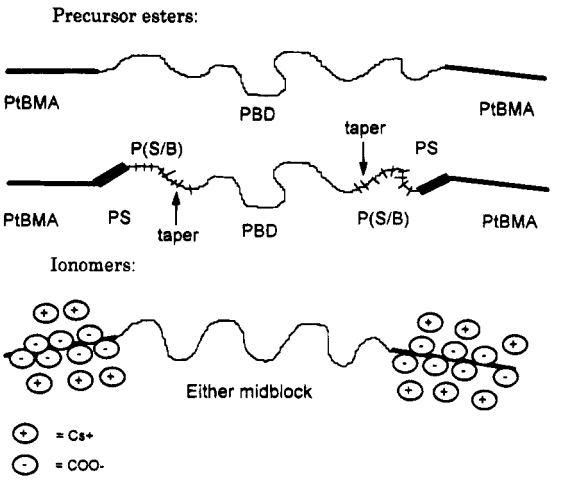

Figure 1. Schematic of the chain architecture for the triblock polymers used in this study.

Experimental Section

These materials were anionically synthesized; the synthesis and characterization have been reported elsewhere.[25,26] Briefly, center blocks were produced from a lithiated difunctional initiator and the appropriate monomer(s) and then quenched, followed by reactivation and subsequent addition of the *tert*-butyl methacrylate (tBMA) end blocks. The center block composition was also varied. In one case, the center block is poly(butadiene) (PBD), with ~60 mol % *trans* configuration. The other center block is a "tapered" triblock like commercial styrene–butadiene rubber (SBR), where the PBD midblock "tapers" outward into the PS ends. There is an illustration of each type of macromolecule in Figure 1, with the specific molecular characteristics of the ester precursors listed in Table 1. After the ester precursor was made, the tBMA end blocks were hydrolyzed using methane/sulfonic acid in 80/20 (v/v) toluene/glacial acetic acid. The resultant methacrylic acid block-terminated polymers were precipitated, dried, and redissolved into 90/10 (v/v) toluene/methanol, for neutralization using methanolic cesium carbonate (0.11 N).[25] Films were formed from the as-neutralized solutions by casting onto Teflon trays and allowing the solutions (~5 wt % polymer) to dry at room temperature. The films were further dried in vacuo at ~90 °C for 12 h to remove residual solvent or water and were stored in a desiccator to avoid potential moisture uptake.

The nomenclature used here is *midblock type-mol %* tBMA (T) *counterion*, so that tSBS-4TCs is a triblock with a tapered S/B/S (SBR) center and 4 mol % tBMA (total) ends, neutralized to form the cesium carboxylate end block. For the nonionic ester precursor, the "Cs" is omitted.

SAXS experiments were performed on a standard Kratky camera, equipped with a Braun position sensitive detector, and supplied with Ni-filtered Cu Kα radiation ($\lambda = 0.154$ nm) by a Philips PW-1729 X-ray generator. Experimental intensities were corrected for sample thickness, absorption, and counting time and were normalized to a Lupolen standard. TEM was performed on a Philips STEM-610 operating at 60 kV on specimens cryomicrotomed in tetramethyldisiloxane. Tetramethyldisiloxane was used due to the very low temperature (~−80 °C) of operation and solubility of the ionic domain in polar solvents, such as ethanol. Staining of the precursor esters for TEM contrast enhancement was done via RuO_4 or OsO_4 vapor, as noted in the associated text. Dynamic mechanical analysis was performed on a Seiko DMS-210 under dry N_2 purge at a heating rate of 2 °C/min.

Results

Small-Angle X-ray Scattering. The slit-smeared SAXS profiles for the precursors and the resultant ionomers are found in Figures 2 and 3, where the log of relative intensity is plotted as a function of the log of the angular variable, s, where $s = (2/\lambda) \sin \theta$ and θ is half the radial scattering angle. The smeared "d"

Table 1. Characteristics of the Triblock Polymers Used in This Study

triblock	center $\bar{M}_n$ (SEC)	tBMA[a] (mol %)	center BD (mol %)	S in taper (mol %)	center $\bar{X}_n$	tBMA $\bar{X}_n$ per end block	end block vol fractn	end block mass fractn
PBD-9T	77 000	9	100.0	0	1424	70	0.16	0.19
PBD-5T	67 600	5	100.0	0	1250	33	0.09	0.11
PBD-4T	78 500	4	100.0	0	1451	30	0.07	0.09
PBD-3T	64 600	3	100.0	0	1194	18	0.05	0.07
tSBS-9T	139 600[b]	9	85.2[c]	63	2271	112	0.14	0.17
tSBS-4T	95 800[b]	4	80.4[c]	70	1499	31	0.06	0.08
tSBS-3T	115 500[b]	3	85.2[c]	67	1879	29	0.05	0.06
tSBS-2T	112 000[b]	2	83.9[c]	61	1802	18	0.03	0.04

[a] As determined by ^{13}C NMR. [b] Uncorrected, versus standards. [c] Weight percent in taper.

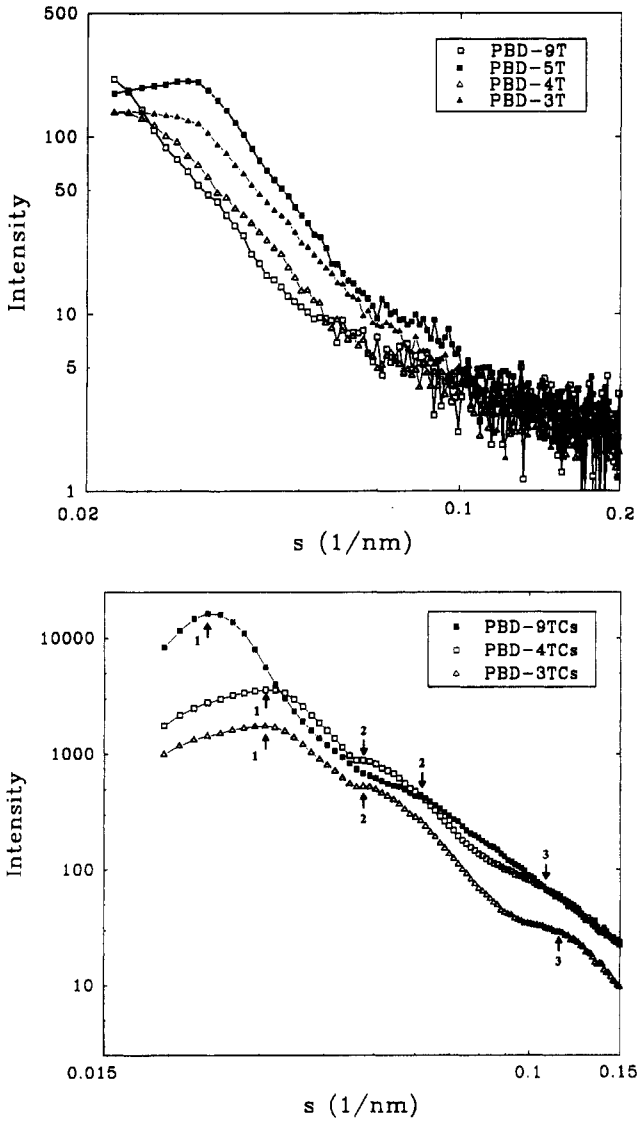

Figure 2. Slit-smeared log I − log s SAXS profiles of (a, top) of the PBD ester precursors and (b, bottom) of the PBD cesium ionomers. Intensity is in arbitrary units.

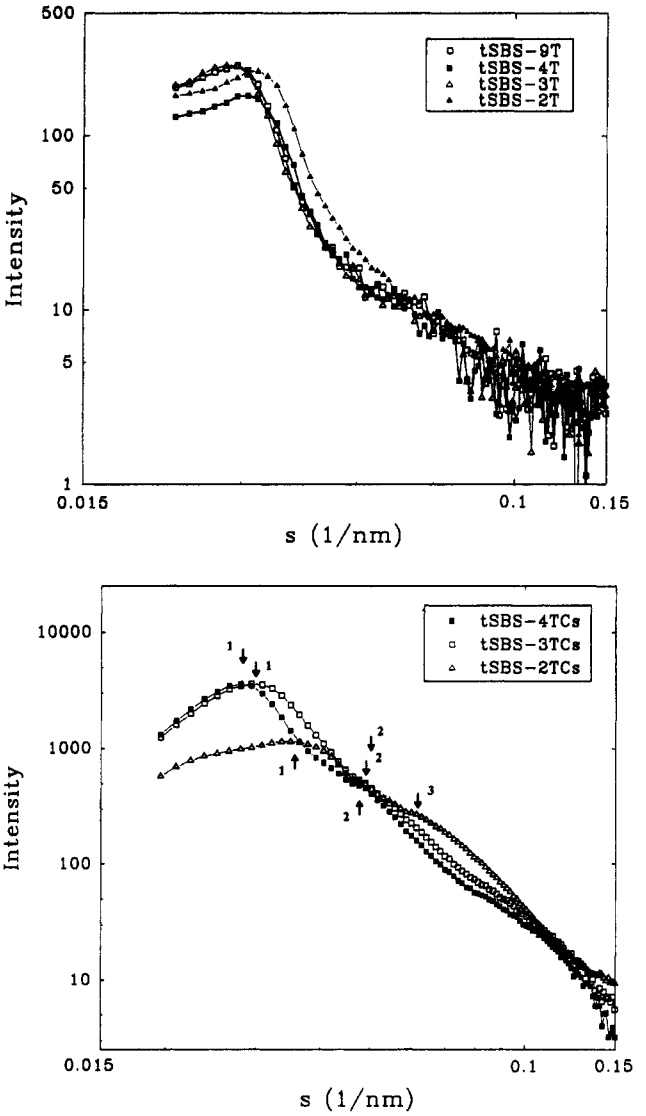

Figure 3. Slit-smeared log I − log s SAXS profiles of (a, top) the tSBS ester precursors and (b, bottom) the tSBS cesium ionomers. Intensity is in arbitrary units.

spacings determined from Bragg's law at the peak SAXS intensities are given in Table 2. Determination of interfacial thickness was not attempted from the terminal region of the SAXS curve due to the presence of multiple peaks and their unknown effect on the terminal SAXS intensity. When peaks lie near one another so that their terminal regions overlap, an accurate value of terminal intensity is not discernable and determination of interfacial thickness is then inaccurate. However, the domains were observed by TEM (discussed later) and so the errors that would have been encountered in interfacial thickness analysis from multiple-peak SAXS curves were avoided.

As can be seen in Figure 2a, the PBD precursors show clear SAXS peaks only in the case of the 3 and 5 mol % tBMA. The 9 mol % precursor exhibits no peak and the 4 mol % precursor only a slight shoulder very near the beam stop, which is not a complete peak. The intensities suggest that the observed peak is due to the aggregation of the PtBMA end blocks into discrete domains in the PBD matrix, since the peak intensity increases from PBD-3T to PBD-5T. Likewise, the intensity at the lowest accessible value of s increases as one goes from PBD-4T to PBD-9T. Although the peak is not observed for PBD-9T, it is expected to be in the beam stop of the camera; TEM indicates that the spacing is at least 50 nm, which is beyond the resolution

Table 2. Smeared SAXS Spacings of the Triblock Copolymers Used in This Study[a]

triblock	precursor (nm)	Cs^+ Ionomer (nm)
PBD-9T	in beam stop	42, 18
PBD-5T	33	na[b]
PBD-4T	in beam stop	33, 21, 10
PBD-3T	32	33, 21, 8.2
tSBS-9T	34	na
tSBS-4T	33	36, 20
tSBS-3T	36	34, 17
tSBS-2T	33	29, 19, 16

[a] The smeared spacings were estimated by Bragg's relation: $s \sim 1/d$, at each peak value of intensity. [b] na, sample not available.

of the Kratky camera employed. The smeared interdomain spacings of the PBD ester precursors (Table 2) do not vary greatly with end block length. The 5 mol % ester precursor exhibits a peak (corresponding to a smeared "d" of 33 nm), as does the 3 mol % precursor (32 nm), whereas the 4 mol % material shows a very broad shoulder-like maximum very close to the beam stop. Table 1 indicates, though, that the center block size is not constant from polymer to polymer, and thus, the interdomain spacings are not expected to change systematically with end block length, even though the molar proportion of the end blocks to the center block is systematically changing. Thus, the peak position is expected to be in the beam stop of our camera due to the high center block number-average molecular weights of PBD-4T (78 500 g/mol) and PBD-9T (77 000 g/mol). These number-average molecular weights are somewhat greater than that of PBD-5T (67 600 g/mol) or of PBD-3T (64 600 g/mol).

In the PBD ionomers, the primary peak intensity does increase with increasing ionic content, i.e., increasing cesium carboxylate end block length. This observation lends credence to the assignment of the primary maximum to the primary interdomain spacing, where the increased intensity is a result of an increase in the concentration of scattering centers, which will also be discussed later in terms of the TEM results. The additional smeared spacings reported in Table 2 for the PBD-Cs^+ ionomers are derived from the shoulders in the SAXS profiles (denoted by arrows and numerals). The presence of these shoulders can be associated with polydispersity in the size distribution of spherical scatterers or shape anisotropy (i.e., longer in one direction than another) of the scatterers.[42] Other researchers have deduced from SAXS profiles the influence of size distribution in a system of spherical ionic scatterers[36] or "elongate" spheroid ionic domains as the dispersed phase in similar triblock ionomers.[34] This question of whether the scattering arises from shape factors or size distribution is addressed further in the later section on TEM. However, one notes that there is an increase in the smeared interdomain spacing in the PBD ionomers as the end block size increases from 3 or 4 to 9 mol %. This increase is observed even in the case where the center blocks are of similar size, as in the 4 and 9 mol % ionomers. There is little difference in the interdomain spacings of the PBD-4TCs and PBD-3TCs ionomers, despite the fact that the $\bar{M}_n$ of the center block in PBD-4TCs is considerably higher than that of PBD-3TCs. Thus, the $\bar{M}_n$ of the ionic end block appears to affect the interdomain spacing more strongly than does the length of the PBD center block, as was also found by Gouin et al.[34,36]

The smeared SAXS profiles of the tSBS precursors are shown in Figure 3. The primary interdomain spacings estimated from the peak values of s are reported in Table 2, which indicates no systematic variation in interdomain spacing with either center block or end block $\bar{M}_n$. Noting the large variation in tSBS center block $\bar{M}_n$ (Table 1), presumably there would be a systematic difference in the interdomain spacing in the tSBS materials as a function of center block $\bar{M}_n$. The reason for the lack of any systematic variation in the smeared interdomain spacing is likely the variable architecture of the tapered center block. Both $\bar{M}_n$ and the amount of incorporated styrene change from one material to the next, and thus, there is no way of specifying exactly how the chain dimensions should vary. Also, the composition of the center block is crucial in these systems because the tapered portion of the center block will tend to affect phase mixing in these systems. Increased length of the taper for the same overall molecule and monomer content will promote less distinct phase separation, as has been shown in SAXS and dynamic mechanical analysis (DMA) from tapered diblock copolymers of styrene and butadiene by Hashimoto et al., for example.[43] This increased phase mixing will be discussed later in the section on TEM. Also note that the intensity of the peaks is not a function of tBMA end block content, as might be expected for a two-phase system of two different electron densities. This lack of end block content dependence suggests that the tapered architecture is affecting the degree of phase separation. In fact, the peak intensity in the tSBS precursors is proportional to the amount of butadiene in the center block (Table 1, column 4). The precursor esters with the highest butadiene (BD) content (tSBS-9T and tSBS-3T, 85 mol %) have the highest peak intensity, and the peak intensity drops slightly as one moves to lower BD content (84 mol %, tSBS-2T) and then drops substantially to the lowest BD composition (80 mol %, tSBS-4T). This would suggest that the incorporation of styrene into the center block decreases the electron density difference (hence, X-ray contrast) between the dispersed phase and the continuous phase and broadens the interphase, thereby lowering the peak intensity.

The smeared SAXS profiles of the tSBS ionomers are shown in Figure 3b. Here, however, there is systematic variation of estimated interdomain spacing with end block length, as shown in Table 2. As the mole percent end block decreases from 4 to 3 to 2, the spacing decreases from 36 to 34 to 29 nm. As in the PBD-based ionomers, this result is in agreement with the findings of Gouin and co-workers,[34,36] who showed that the end block length in similar triblock ionomers strongly affected interdomain spacing, much more strongly than the center block length. The moderate decrease in the interdomain spacing from tSBS-4TCs to tSBS-3TCs is likely due to the accompanying increase in the center block $\bar{M}_n$, and the dramatic decrease in d from tSBS-3TCs to tSBS-2TCs is due to the combined effect of a slight decrease in $\bar{M}_n$ of the center block and a 30% decrease in the amount of the end block cesium carboxylate units. In addition, the secondary shoulders in the SAXS profile indicate, again, some periodicity or that a shape factor is affecting the system scattering, which will be addressed below. The peak intensity of the scattering from the cesium ionomers decreases with ionic content, allowing for the fact that tSBS-3TCs was overneutralized to 135% of end point and that the excess neutralizing agent was not removed from the system.[26] The peak intensity of the ionomers is not affected by the styrene content in the taper, unlike the ester precursors. The effect of styrene content in the taper on either the X-ray contrast or the interphase width

would be minimal compared to the enhancement afforded by Cs^+.

Transmission Electron Microscopy. SAXS indicated that these materials have phase-separated morphologies, and TEM was performed on select materials. The ionomers were photographed unstained, and the precursor esters were stained with either RuO_4 or OsO_4. In each case, the focus was carefully optimized and photographs of a few regions were taken in each of several specimens to ensure that the TEMs reflect the actual system morphology.

In Figure 4a and b, the morphologies of the PBD precursors and ionomers, respectively, are shown in representative TEMs. In Figure 4a and b, one can see that the morphology of PBD-9T changes drastically from that of dispersed rods or lamellae of ~15 nm thickness and ~53 nm center to center in the precursor ester to that of dispersed spheroids in the ionomer. In Figure 4a, the precursor was stained for 0.5 h with RuO_4, a selective stain for unsaturated groups, as in PBD, but does not react with (stain) ester functionalities,[44] as in PtBMA. Thus, the dark phase is PBD and the light phase PtBMA. Note that there are no rod "ends" visible in Figure 4a; however, in (c), a lower magnification TEM of the same area of the RuO_4-stained precursor, one sees a few regions where some ends are visible, such as the region denoted by an arrow. Note also that the volume fraction (~16%, Table 1) of the PtBMA end blocks in the PBD-9T material suggests that the morphology should be dispersed rods and not lamellae. Lamellae are typically found in the morphology of nonionic block copolymers at volume fractions of ~35–65%. In Figure 4b, spherical ionic domains of ~40 nm diameter and ~53 nm center to center are observed in the cesium salt of the PBD-9T material. The ionic domains are also slightly aggregated in the matrix, as semicontinuous regions of lighter colored PBD are clearly visible between the spheroids. It should be noted that the esters were cast from a cyclohexane/THF/methanol [~45/45/10(v/v/v)] solvent in contrast to the casting solvent of the ionomer which is 90/10 (v/v) toluene/methanol initially plus large amounts of THF used to prevent gelation during the neutralization.[26] Thus, it is not certain that the morphological transformation is due solely to the neutralization of the end blocks, and the transformation could also be influenced by a solvent effect. Still, it may be that the Flory–Huggins parameter is much larger for the ionomer versus the precursor and that greater phase segregation is therefore favored, promoting the formation of ionic spheroids and not rodlike domains. Whatever the cause, it will be shown that this morphological transformation has pronounced consequences in the properties of these systems. The TEM images of the other esters and ionomers are not given here for brevity, but both the precursor esters and ionomers exhibited spherical dispersed phases. The other precursors exhibited spherical dispersed phases presumably because of the lower volume fraction of PtBMA versus PBD-9T (Table 1). The size of the PtBMA and cesium carboxylate domains decreased with decreasing PtBMA $\bar{M}_n$ as would be expected. Again, the ionic domains appeared to aggregate together in the matrix, as in PBD-9TCs, with the lighter colored PBD matrix material semicontinuous around the aggregates of 4–6 spheroids.

The TEM of the tSBS-3T materials also produced interesting results, as shown in Figure 5. As part a shows, there is ordering of larger aggregates on the scale of ~35–40 nm in diameter, with more darkly stained regions of ~5–10 nm embedded in lighter stained material composing the large aggregates. The question naturally arises as to the origin of the smaller, dark

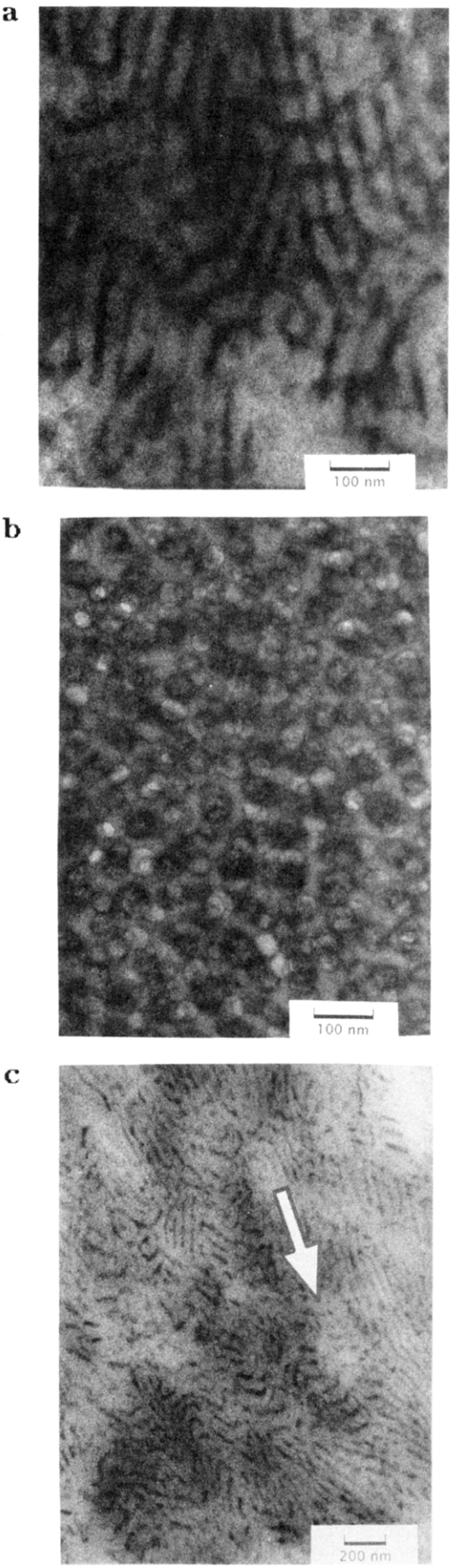

Figure 4. Transmission electron micrographs of PBD-9T triblocks: (a) PBD-9T ester stained with RuO_4; (b) PBD-9TCs; (c) lower-magnification TEM of PBD-9TCs showing ends of cylinders (arrow).

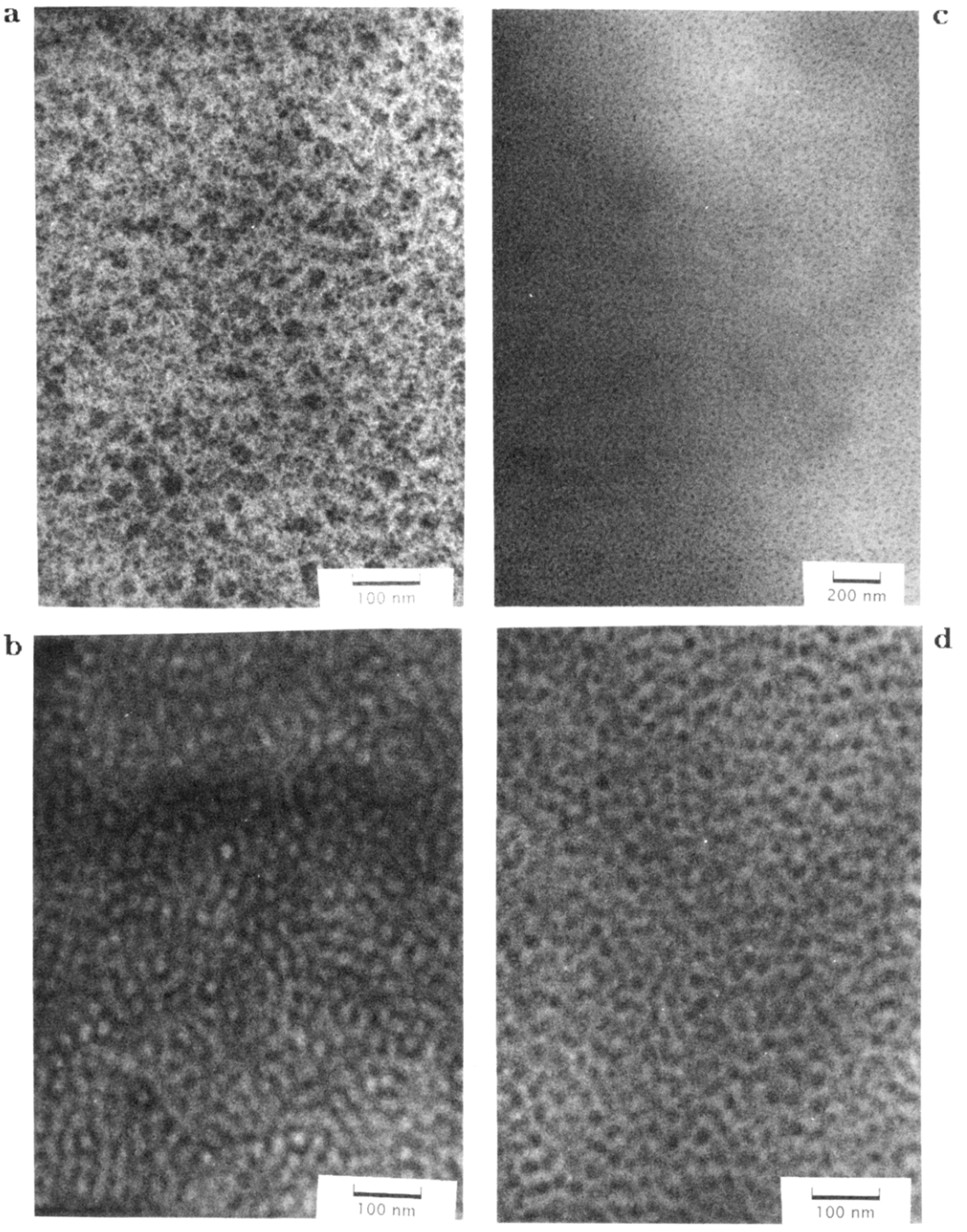

Figure 5. Transmission electron micrographs of tSBS triblocks: (a) tSBS-3T RuO_4-stained for 30 min; (b) tSBS-3T OsO_4-stained for 30 min; (c) tSBS-3TCs; (d) tSBS-3TCs at higher magnification than (c).

regions in the larger aggregates in Figure 5a (RuO_4-stained precursor). This type of morphology is found in all the tSBS precursors examined; the sizes of the large and small regions change only slightly. The morphology can perhaps be explained by a comparison utilizing RuO_4 and the other staining agent, OsO_4. Note Figure 5b, where the OsO_4 is the stain that differentiates the PBD and dispersed PS/tBMA regions and not necessarily the individual components of the PtBMA/PS phase. The lack of "spots" within the lighter stained regions is due to the fact that the OsO_4 oxidizes very slowly relative to RuO_4, which rapidly oxidizes both aromatic and unsaturated moieties.[44] Thus, RuO_4 easily and rapidly (relative to OsO_4) stains PBD and PS, though not PtBMA,[44] and the dark spots of 5−10 nm in diameter in Figure 5a *could* be the PS-rich portion of the PS/PtBMA end block mixed phase. On the other hand, the small, dark spots could also be due to differences in the diffusion rate of the RuO_4 into the TEM specimen, as well. If the dark regions in (b) are taken to be the PBD midblock, then the fading of the dark into the light regions is possibly caused by the tapering of the center block from the PBD midblock to the PS portions. In this particular case, the light regions are ~16 nm in diameter and ~25−30 nm (center to center) apart. The tSBS-3T TEM interdomain spacing agrees reasonably well with the number from SAXS (36 nm). Given that the dark regions are PBD, the degree of phase mixing in the tSBS precursors would thus appear to be significant, as predicted by looking at Table 1 and which was addressed earlier in regard to SAXS. Given that the dark-to-light fading of the staining represents the transition from PBD to PS, TEM gives additional evidence that the interphase region is broad. This broad interphase is encouraged between the immiscible homopolymer ends of the molecule due

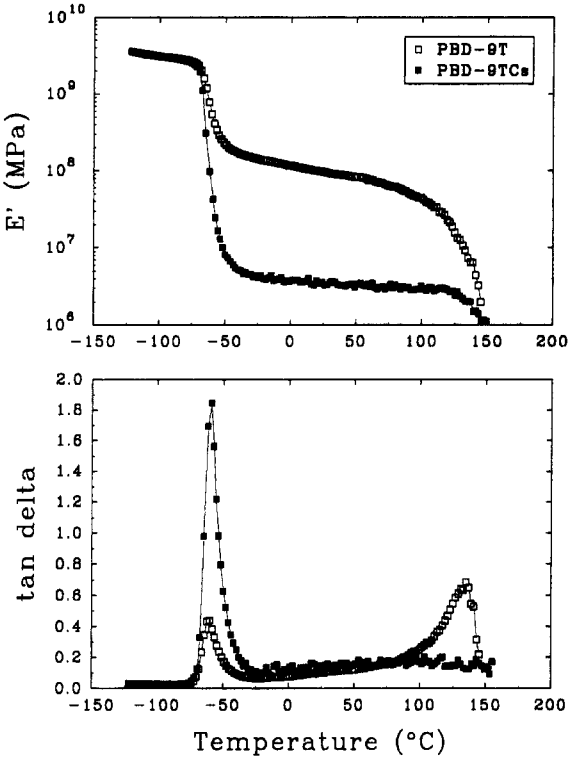

Figure 6. Dynamic mechanical analysis of PBD-9T and PBD-9TCs.

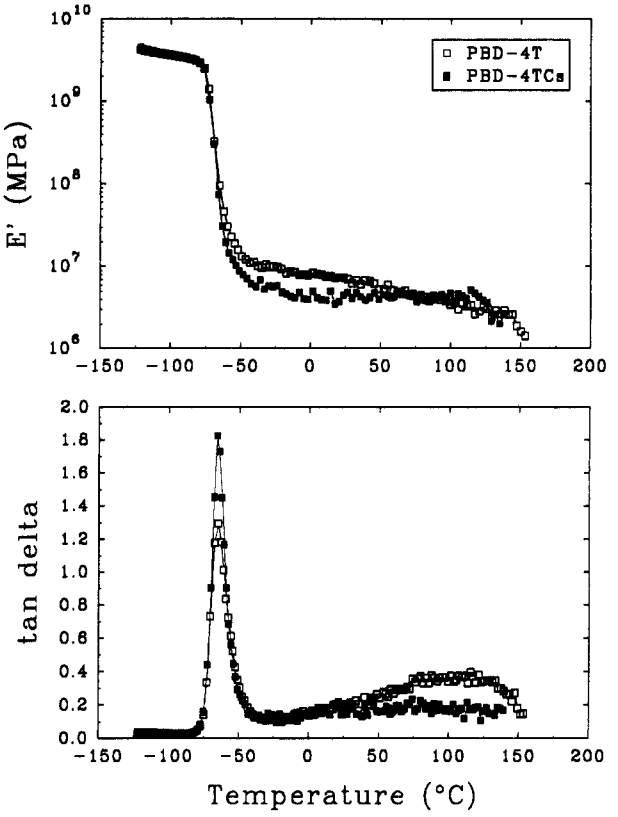

Figure 7. Dynamic mechanical analysis of PBD-4T and PBD-4TCs.

to the good miscibility of the statistically tapered portions of the molecule. As noted before, this tapering miscibility effect was also seen by Hashimoto et al.[43] in PS/PBD diblocks. Thus, in the micrograph there is a gradual fading of the dark to the light regions, because the PBD content is gradually decreasing. The effect of ionization can be seen clearly by comparing parts a and d of Figure 5. The ionomers, shown in (c) and (d), exhibit aggregations of ionic domains that are 25–50 nm apart (center to center) and composed of small ionic spheroids of ~10 nm diameter. Particular attention should be called to (d), a higher magnification TEM, which shows the aggregation of the small ionic spheroids near one another to form the aggregations mentioned above. Thus, it would appear that the ionic spheroids form when cast from solution and then aggregate preferentially in the nonionic matrix, in a fashion similar to random ionomers, where multiplets are pictured as coalescing into clusters of ionic domains.

Dynamic Mechanical Analysis. Dynamic mechanical analyses of PBD-9T and PBD-9TCs are shown in Figure 6. It is apparent from the DMA that there is a very significant difference in the ester precursor and the corresponding ionomer, as anticipated. TEM indicated that the PBD-9T material has a dispersed rodlike morphology and that the PBD-9TCs material has dispersed ionic spheroids which are aggregated together in the PBD matrix. Thus, the upper curve is that of a two-phase system, but the modulus is higher than that of the PBD center block, because the PtBMA domains are continuous and are glassy up to ~100 °C. The transformation from continuous to dispersed domains is very apparent from the change in E' at the glass transition, with the drop in E' being much smaller in the ester than the ionomer due to the lower rubbery modulus of the continuous PBD matrix in the ionomer. The loss peak at the dynamic mechanical glass transition temperature (T_g, ~−65 °C) indicates much more dramatic damping in the ionomer than the ester as well. The peak of the high-temperature dispersion associated with the T_g of the PtBMA domains (~120 °C) disappears upon ionization, indicating a conversion of the PtBMA end blocks to cesium carboxylate. Note that the transition from rubbery to viscous flow behavior moves from ~75 to ~125 °C upon ionization, as well, implying that the dispersion is just very broad and that the ionomer loses mechanical integrity at ~125 °C. In Figure 7, note that the difference in the PBD-4T ester and cesium ionomer is not nearly so pronounced in the 9 mol % materials, where the neutralization resulted in a major change in morphology. Recall that TEM showed that the 4 mol% materials have spheroid morphologies, yet it is still seen that the modulus drop at the T_g (~−65 °C) and the magnitude of the tan δ peak are smaller in the ester than the ionomer. This difference is thought to be a result of more phase mixing in the ester versus the ionomer, which would tend to raise the T_g of the system. Also note that the tan δ dispersion at higher temperatures (broad and centered at ~110 °C) disappears upon neutralization, though the dispersion was already less pronounced in PBD-4T versus PBD-9T, owing to the PtBMA phase continuity in the PBD-9T system.

The tapered SBS systems, on the other hand, are not so straightforward in terms of interpretation of their dynamic mechanical behavior, due to structure. Figure 8 shows the dynamic mechanical profiles of the ester precursors for the tSBS systems. All the materials suggest two-phase behavior, and three of the four materials show essentially the same glass transition behavior. The reason that tSBS-4T does not have the same T_g as the other tSBS materials is shown in Table 3, where one sees that the PBD midblock of the tSBS-4T center block is a much smaller fraction of the total center block than in the other esters. The ratio of the amount of elastomeric PBD midblock to the amount of higher T_g styrene–butadiene taper segments is distinctly smaller (about half) in the tSBS-4T material than

Table 3. Characteristics of the tSBS Center Block Copolymers Used in This Study

triblock	S in taper (mol %)	total no. of S units	$\bar{X}_n$ of PS end block	no. of BD units	homo-PBD/total BD in triblock	homo-PBD/ S−B taper
tSBS-9T	63	335	124	1936	0.89:1	4.1:1
tSBS-4T	70	294	88	1204	0.83:1	2.4:1
tSBS-3T	67	277	91	1601	0.88:1	3.8:1
tSBS-2T	61	290	113	1512	0.88:1	3.8:1

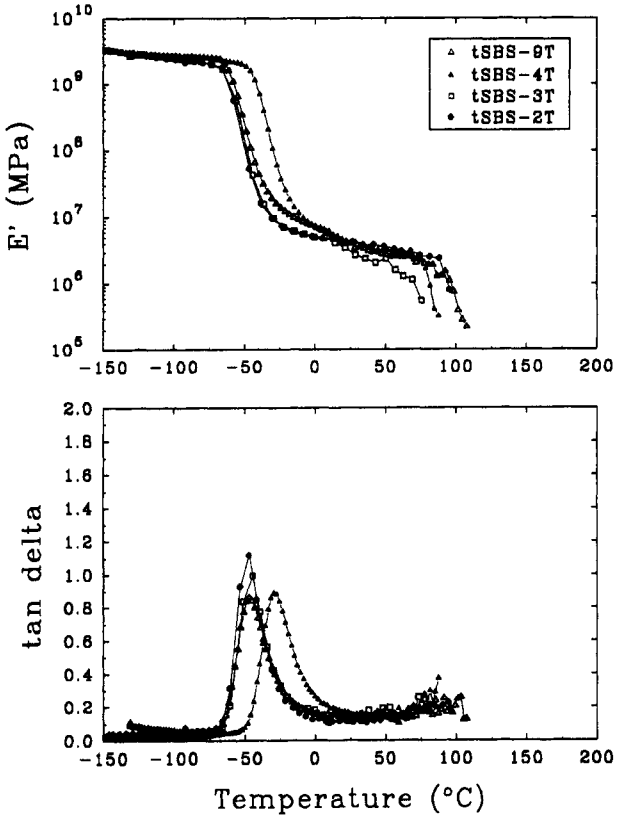

Figure 8. Dynamic mechanical analysis of tSBS precursor esters.

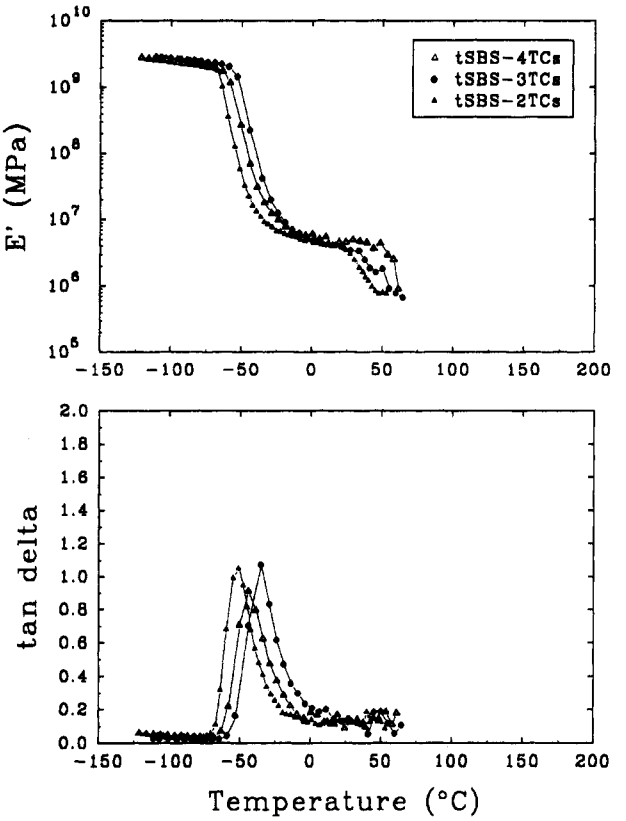

Figure 9. Dynamic mechanical analysis of tSBS cesium ionomers.

in the others, as shown in the last column. Thus, the glass transition process in the tSBS-4T ester will occur at a somewhat higher temperature because the center block has a higher overall T_g. In the case of the tSBS-2T and tSBS-3T materials, there is essentially no difference in their center block compositions and their glass transition behavior is similar. The softening transition above room temperature appears to vary randomly from material to material. A tentative explanation, which is supported by the TEM evidence from the RuO_4-stained materials, would be that the PS and PtBMA blocks are a mixed phase, and therefore, only a single transition in E' is seen, over the range of 50−~90 °C, depending on the ester chosen. This mixing would appear to be the cause, since the two esters with the highest number of PS + PtBMA units, tSBS-2T (150 units) and tSBS-9T (235 units), persist to higher temperatures before flowing than the two lowest, tSBS-4T and tSBS-3T (both 120 units). These differences in the number of end block repeat units are significant, as these are small blocks where 30 units amount to 25% of the total end block repeat units.

The DMAs of the tSBS-based cesium ionomers are found in Figure 9 and show that the glass transition behavior is similar to the ester precursors, again allowing for the extra neutralization (to 135%) of tSBS-3TCs. The glass transition temperatures of each ionomer are very similar, and the tan δ dispersion is not sharpened or narrowed by neutralization, unlike the PBD-center block materials. The tapered center block architecture appears to have broadened the glass transition region considerably in the ionomer just as in the precursor (Figure 8). Interestingly, the flow transition is found at lower temperatures in the cesium ionomers than in the ester precursors. This may be the result of residual solvent or water, though precautions were taken to ensure dry conditions and specimens. As a final observation, it was noted in the ionomers that longer cesium carboxylate end blocks yield higher flow transition temperatures, as would be expected from the increased volume fraction of the less mobile ionic phase.

Conclusions

The morphological structure and properties of a series of triblock copolymers from poly(tBMA-*b*-BD-*b*-tBMA) or poly(tBMA-*b*-S-*t*-BD-*t*-S-*b*-tBMA) (tBMA = *tert*-butyl methacrylate; BD = butadiene; S = styrene; *t* = taper) and the corresponding cesium ionomers have been described. It has been shown that the materials containing poly(butadiene) center blocks are easily understood in terms of the current knowledge of block copolymer ionomers. Upon neutralization, the PBD-9T material underwent a morphological transformation from a rodlike morphology to dispersed, ionic spheres. This transition was evident from the TEM and DMA results of the respective materials. Neutralization promotes stronger phase separation even when the morphology does not change, as shown by the DMA of the PBD-4T material. The SAXS results correlate well with the TEM data for the PBD precursor esters and

cesium ionomers. The SAXS results also indicate some systematic, explicable change in the observed interdomain spacings, as the measured interdomain spacing varies with center block $\bar{M}_n$. TEM shows that the ionomer consists of small, ionic spheroids aggregated throughout the PBD matrix. There is a slight connectivity of ionic domains in PBD over intermediate distances (less than ~150 nm).

On the other hand, the interpretation of the results for the tapered SBS materials is not straightforward. Precursor SAXS peak intensity was found to be a function of butadiene content in the center block, though a systematic change in interdomain spacing was not observed. Upon neutralization, however, the smeared interdomain spacing was shown to decrease with increasing $\bar{M}_n$ of the ionic end block. Although neutralization improves phase separation noticeably in PBD materials, it has a less noticeable effect in the tSBS materials. TEM indicates that the tapering of the midblock in the tSBS ester precursors enhances the phase mixing in the precursors and apparently has no effect on the ionomer morphology, which exhibited dispersed ionic spheroids like the PBD-based materials. TEM shows clearly that the morphology of the tSBS ionomer is that of aggregates of small (5–10 nm) ionic spheroids with the aggregates of the spheroids being ~50–70 nm in size. The microstructure of the center block is given as the basis for the glass transition behavior of the precursor, and the end blocks (both PS and PtBMA) are responsible for the transition to flow. The glass transition in the tSBS ionomers is not sharpened or narrowed versus the ester precursor, as in the PBD ionomers, for which the tapering of the center block is responsible. Additionally, the transition to flow moves to higher temperature as the length of the ionic end block increases in the tSBS ionomers.

Acknowledgment. Partial support of this work from the Gencorp Foundation is greatly appreciated.

References and Notes

(1) Eisenberg, A. *Macromolecules* **1970**, *3*, 147.
(2) MacKnight, W. J.; Taggart, T. P.; Stein, R. S. *J. Polym. Sci., Polym. Symp.* **1974**, *45*, 113.
(3) Fujimura, M.; Hashimoto, T.; Kawai, H. *Macromolecules* **1982**, *15*, 136.
(4) Forsman, W. C. *Macromolecules* **1982**, *15*, 1032.
(5) Yarusso, D. J.; Cooper, S. L. *Macromolecules* **1983**, *16*, 1871.
(6) Yarusso, D. J.; Cooper, S. L. *Polymer* **1985**, *26*, 371.
(7) Lee, D.; Register, R. A.; Yang, C.; Cooper, S. L. *Macromolecules* **1988**, *21*, 998.
(8) Mauritz, K. A. *J. Macromol. Sci. Rev. Macromol. Chem. Phys.* **1988**, *C28*, 65.
(9) Eisenberg, A.; Hird, B.; Moore, R. B. *Macromolecules* **1990**, *23*, 4098.
(10) (a) Broze, G.; Jérôme, R.; Teyssié, Ph. *Macromolecules* **1981**, *14*, 224. (b) Broze, G.; Jérôme, R.; Teyssié, Ph. *Macromolecules* **1982**, *15*, 1300.
(11) (a) Mohajer, Y.; Tyagi, D.; Wilkes, G. L.; Storey, R. F.; Kennedy, J. P. *Polym. Bull.* **1982**, *8*, 47. (b) Bagrodia, S.; Mohajer, Y.; Wilkes, G. L.; Storey, R. F.; Kennedy, J. P. *Polym. Bull.* **1982**, *8*, 281. (c) Bagrodia, S.; Mohajer, Y.; Wilkes, G. L.; Storey, R. F.; Kennedy, J. P. *Polym. Bull.* **1983**, *9*, 174.
(12) Storey, R. F.; George, S. E.; Nelson, M. E. *Macromolecules* **1991**, *24*, 2920.
(13) Storey, R. F.; Lee, Y. *J. Polym. Sci. A: Polym. Chem.* **1991**, *29*, 317.
(14) Venkateshwaran, L. N.; Tant, M. R.; Wilkes, G. L.; Charlier, P.; Jérôme, R. *Macromolecules* **1992**, *25*, 3996.
(15) Feng, D.; Wilkes, G. L.; Leir, C. M.; Stark, J. E. *J. Macromol. Sci.–Chem.* **1989**, *A26*, 1151.
(16) Feng, D.; Venkateshwaran, L. N.; Wilkes, G. L.; Leir, C. M.; Stark, J. E. *J. Appl. Polym. Sci.* **1989**, *37*, 1549.
(17) Venkateshwaran, L. N.; Wilkes, G. L.; Leir, C. M.; Stark, J. E. *J. Appl. Polym. Sci.* **1991**, *43*, 951.
(18) Allen, R. D.; Long, T. E.; McGrath, J. E. *Polym. Bull.* **1986**, *15*, 127.
(19) Allen, R. D.; Yilgor, I.; McGrath, J. E. In *Coulombic Interactions in Macromolecular Systems*; Eisenberg, A., Bailey, F. E., Eds.; ACS Symposium Series 302; American Chemical Society: Washington, DC, 1986.
(20) Long, T. E.; Deporter, C. D.; Patel, N.; Dwight, D. W.; Wilkes, G. L.; McGrath, J. E. *Polym. Prepr. (Am. Chem. Soc., Div. Polym. Chem.)* **1987**, *28*, 214.
(21) Deporter, C. D.; Long, T. E.; Venkateshwaran, L. N.; Wilkes, G. L.; McGrath, J. E. *Polym. Prepr. (Am. Chem. Soc., Div. Polym. Chem.)* **1988**, *29*, 343.
(22) Long, T. E.; Allen, R. D.; McGrath, J. E. In *Chemical Reactions on Polymers*; Benham, J. L., Kinstle, J., Eds.; American Chemical Society: Washington, DC, 1988.
(23) McGrath, J. E.; DeSimone, J. M.; Hellstern, A. M.; Hoover, J. M.; Broske, A. D.; Long, T. E.; Smith, S. D.; Cho, C.; Yu, Y.; Wood, P.; Deporter, C. D.; Riffe, J. S. In *Multiphase Macromolecular Systems*, Culbertson, B. M., Ed.; Plenum Press: New York, 1989.
(24) Deporter, C. D.; Long, T. E.; McGrath, J. E. *Polym. Int.* **1994**, *33*, 205.
(25) Deporter, C. D.; Ferrence, G. M.; McGrath, J. E. *Polym. Prepr. (Am. Chem. Soc., Div. Polym. Chem.)* **1993**, *34*, 574.
(26) Deporter, C. D. Ph.D. Dissertation, Virginia Polytechnic Institute and State University, Blacksburg, VA, 1991.
(27) Venkateshwaran, L. N.; York, G. A.; DePorter, C. D.; McGrath, J. E.; Wilkes, G. L. *Polym. Prepr. (Am. Chem. Soc., Div. Polym. Chem.)* **1989**, *30*, 248.
(28) Venkateshwaran, L. N.; York, G. A.; Deporter, C. D.; McGrath, J. E.; Wilkes, G. L. *Polymer* **1992**, *33*, 2277.
(29) Ramireddy, C.; Tuzar, Z.; Procházka, K.; Webber, S. E.; Munk, P. *Macromolecules* **1992**, *25*, 2541.
(30) Munk, P.; Ramireddy, C.; Tian, M.; Webber, S. E.; Procházka, K.; Tuzar, Z. *Makromol. Chem., Macromol. Symp.* **1992**, *58* (Solution Prop. Modif. Polym.), 195.
(31) Procházka, K.; Kiserow, D.; Ramireddy, C.; Webber, S. E.; Munk, P.; Tuzar, Z. *Makromol. Chem., Macromol. Symp.* **1992**, *58* (Solution Prop. Modif. Polym.), 201.
(32) Gauthier, S.; Eisenberg, A. *Macromolecules* **1987**, *20*, 760.
(33) Wollmann, D.; Williams, C. E.; Eisenberg, A. *J. Polym. Sci.: B: Polym. Phys.* **1990**, *28*, 1979.
(34) Gouin, J.-P.; Williams, C. E.; Eisenberg, A. *Macromolecules* **1989**, *22*, 4573.
(35) Gouin, J.-P.; Williams, C. E.; Eisenberg, A. *Macromolecules* **1992**, *25*, 1368.
(36) Gouin, J.-P.; Bossé, F.; Nguyen, D.; Williams, C. E.; Eisenberg, A. *Macromolecules* **1993**, *26*, 7250.
(37) Desjardins, A.; Eisenberg, A. *Plast. Rubber Comp. Process. Appl.* **1992**, *18*, 161.
(38) Weiss, R. A.; Sen, A.; Pottick, L. A.; Willis, C. L. *Polymer* **1990**, *31*, 220.
(39) Weiss, R. A.; Sen, A.; Willis, C. L.; Pottick, L. A. *Polymer* **1991**, *32*, 1867.
(40) Weiss, R. A.; Sen, A.; Pottick, L. A.; Willis, C. L. *Polymer* **1991**, *32*, 2785.
(41) Lu, X.; Steckle, W. P.; Weiss, R. A. *Macromolecules* **1993**, *26*, 5876.
(42) Glatter, O.; Kratky, O. *Small Angle X-ray Scattering*; Academic Press: New York, 1982.
(43) Hashimoto, T.; Tsukahara, Y.; Tachi, K.; Kawai, H. *Macromolecules* **1983**, *16*, 648.
(44) Trent, J. S.; Scheinbeim, J. L.; Couchman, P. R. *Macromolecules* **1983**, *16*, 589.

MA946396E